Inversion of velocity models using genetic algorithm method with sigmoidal parameterization

Inversão de campos de velocidade usando o algoritmo genético com parametrização sigmoidal

Juarez dos Santos Azevedo[1]; Lucas Farias Palma[2]

Abstract

A seismic traveltime inversion method is proposed for building smooth velocity models using traveltime observed on irregular surface. Model parameterization in this study is described by a piecewise constant velocity field on a rectangular grid parameterized by sigmodal functions, which is beneficial for the description of irregular surface with high degree of approximation. The velocity field is defined in the rectangular grid which is used for the description of velocity distribution everywhere in the model sigmoidal interpolation. In addition, we use the simple Genetic Algorithm for the inversion procedure. Through this global scope inversion method, we provide high-resolution estimates of the model parameter and ensure that the results obtained are in accordance with the actual data. Our method is validated with synthetic examples of heterogeneous isotropic media and compared to Simulating Annealing. The inverted velocity models and approximate ray paths obtained coincide well with the trajectories simulated using the seismic ray tracing in synthetic heterogeneous isotropic media.

Keywords: seismic Inversion; genetic algorithm; ray tracing; sigmoidal functions; velocity field parameterization.

Resumo

Um método de inversão do tempo de trânsito sísmico é proposto para a estimativa de modelos de velocidades suaves usando o tempo de trânsito observado em superfícies irregulares. A parametrização do modelo neste estudo é descrita por um conjunto de blocos baseado na parametrização por funções sigmoidais de campos de velocidades descontínuos, o que é benéfico para a descrição de superfícies irregulares com alto grau de aproximação. O campo de velocidade é definido na forma de malha retangular que é usado para a descrição da distribuição de velocidades em toda a interpolação sigmoidal do modelo. Além disso, usamos o simples Algoritmo Genético (escopo global) para o procedimento de inversão. Por meio desse método de inversão, fornecemos estimativas de alta resolução dos parâmetros do modelo e garantimos que os resultados obtidos estejam de acordo com os dados reais. Nosso método é validado com exemplos sintéticos de meios isotrópicos heterogêneos e comparados com o Simulating Annealing. Os modelos de velocidade invertida e as trajetórias aproximadas dos raios obtidos coincidem bem com trajetórias simuladas em meios isotrópicos heterogêneos sintéticos.

Palavras-chave: Inversão sísmica; algoritmo genético; traçamento de raios; funções sigmoidais; parametrização de campos de velocidades.

[1] Prof. Dr., ICTI, Universidade Federal da Bahia, Camaçari, Bahia, Brazil, E-mail: jdazevedo@ufba.br
[2] PhD student in CPGG, Universidade Federal da Bahia, Salvador, Bahia, Brazil, E-mail: palma.lucas@ufba.br

17

Semina: Ciênc. Ex. Tech., Londrina, v. 43, n. 1Esp, p. 17-28, Jan./Dez. 2022

Introduction

The imaging of subsurface structures to obtain information on stratigraphic features and structures in geological fields requires the determination of the field of propagation velocities of the seismic waves at each subsurface position. Obtaining this velocity field has been constantly researched in the applied geophysical and represents a crucial part of techniques, such as: seismic tomography (BOZDAĞ; TRAMPERT; TROMP, 2011; CERQUEIRA; FIGUEIRÓ; CUNHA, 2016; RAWLINSON *et al.*, 2014), seismic migration (MENKE, 2012), full waveform inversion (DATTA; SEN, 2016; JIN; CAO; YIN, 2020; SAJEVA *et al.*, 2016), ray tracing (HANYGA; SEREDYŃSKA, 2020), and among others (ELY; MALCOLM; POLIANNIKOV, 2018; MOLLEHUARA-CANALES *et al.*, 2021; STUART; MINKOFF; PEREIRA, 2019).

The main goal of this paper is to combine a genetic algorithm (GA) with a nonlinear inversion scheme using a sigmoidal parameterization to develop velocity fields through ray tracing. By joining GA global scheme and ray tracing, we intend to (i) estimate a good initial model of the velocity field by inversion and (ii) understand the dependence of GA with sigmoidal parameterization. Both techniques has been widespread in literature (DOCHERTY *et al.*, 1997; FERREIRA; PORSANI; OLIVEIRA, 2003; REZAIE, 2020; SAMBRIDGE; DRIJKONINGEN, 1992) and will be used to determine the velocity field coefficients given by the sigmoidal parameterization making this work a novelty. This methodology is useful since it can be applied to any set of traveltimes where forward modeling is effective, regardless of the model geometry or data set to be used. Recently the forward problem of discontinuous velocity fields by sigmoidal parameterization was used by Oliveira *et al.* (2021). This strategy allows sharp variations of the velocity model without neglecting continuity, besides it does not need domain decomposition.

The parameterization of the model performed here is done using rectangular elements. Regardless of mesh type, this kind of parameterization has good adjustability in the discontinuous model since its approximation strongly depends on the sigmoidal parameter, which requires no additional computational cost, especially for complex models whose difficulty in representing the discontinuity with a fine mesh is inherent.

To use the inversion methodology, we first obtain the observed synthetic data through the forward problem and then the inversion is performed in order to obtain a model as close as possible to the target model.

In forward problem, the work consisted of the artificial generation of synthetic profiles of traveltimes. To this end, we calculate the traveltimes of the first arrival of compressional waves from a source and record them on strategically positioned surface receivers. To obtain these times, seismic ray tracing was used, computationally simulating the propagation of waves in an isotropic and heterogeneous geological environment represented by the parameterized velocity fields. In this case, the ray trajectories through the model are traced with a take-off angle uniformly distributed in a given interval from a single surface source. Traveltimes are calculated on such ray trajectories.

In the inverse problem, we use the genetic algorithm to estimate the parameters of the models that best suit the synthetic data of traveltime, i.e, that minimize the difference between the observed synthetic data and the computed data in the current models of the iterative process. Also at this stage, the quality of the results and the application of the inversion method itself were analyzed and discussed.

Here is an outline of the paper. First section, we introduce parameterization by sigmoidal functions. In second section, we present a brief summary of the theoretical foundations of ray tracing and the calculation of traveltimes. The third section describes the implementation of the GA, while in the last section we discuss the results from three numerical examples, comparing them with the Simulated Annealing method (SEN; STOFFA, 2013).

Model parameterization

In order to parameterize the velocity field, we describe a seismic model as an aggregate of arbitrarily shaped cells separated by smoothed interfaces. These cells are provided with different geologic attributes, and their structure is interpolated through sigmoidal functions. The velocities between different interfaces are pieced together by a series of the sigmodal functions involving rectangular cells can be used to simulate the field on a complicated velocity distribution of a *n*-dimensional media.

In this sense, following the notation of Oliveira *et al.* (2021) we approximate the one-dimensional velocity field $v(z)$ as follows:

$$v_a(z) = \sum_{n=-1}^{N} v_n \phi_a\left(\frac{z}{h} - n\right), \qquad (1)$$

where

$$\phi_a(x) = \frac{1}{1 + e^{-ax}} - \frac{1}{1 + e^{-a(x-1)}}, \qquad (2)$$

and a represents the parameter that controls the transition between plateaus, which may be smooth or sharp if a is small or large, respectively.

We can make an extension of equation (1) in rectangular domain $[0, L_x] \times [0, L_z]$ with grid points $(x_m, z_n) = (mh_x, nh_z)$, $0 \le m \le N_x$ and $0 \le n \le N_z$ as follow:

$$v_a(x,z) = \sum_{n=-1}^{N_z} \sum_{m=-1}^{N_x} v_{m,n} \phi_a\left(\frac{x}{h_x} - m\right) \phi_a\left(\frac{z}{h_z} - n\right). \qquad (3)$$

The above expansion can be approximated as:

$$v_a(x,z) \approx \sum_{i=-1}^{1} \sum_{j=-1}^{1} v_{m+i,n+j} \phi_a\left(\frac{x}{h_x} - (m+i)\right) \\ \phi_a\left(\frac{z}{h_z} - (n+j)\right), \qquad (4)$$

where $(x,z) \in [x_m, x_{m+1}] \times [z_n, z_{n+1}]$ and the summation limits may be modified to guarantee $0 \le m+i \le N_x$ and $0 \le n+j \le N_z$.

Note that the parameterization involving rectangular meshes is very flexible for modeling the interfaces. Beyond that, each of the blocks is treated as a homogeneous medium in which the raypath is a straight line.

Ray tracing in heterogeneous models

According to Fermat's Principle (ČERVENÝ, 2001), the trajectory from source A to receiver B on two-dimensional is considered to traversed by the wave is such that the traveltime of the wave propagation is a minimum. This traveltime through of the velocity model V can be calculated using the line integral equation given by

$$T_{AB} = \int_{\mathbf{l}_{AB}} \frac{1}{V(\mathbf{l})} d\mathbf{l} \qquad (5)$$

where $V(\mathbf{l})$ is the (unknown) local velocity along (the unknown) actual ray path $\mathbf{l}_{AB}$ between A and B, which is calculated numerically by the following equation:

$$T_{AB} = \sum_{i=0}^{N} \Delta T_i = \sum_{i=0}^{N} \frac{1}{V_i} \|\mathbf{x}_{i+1} - \mathbf{x}_i\|_2 \qquad (6)$$

such that V_i represents the wave velocity at position $\mathbf{x}_i = (x_i, z_i)$. Therefore, traveltime is a linear combination of reciprocal of velocity.

The ray tracing method derives from the particular solution of the following system of ray equations:

$$\begin{cases} \dfrac{d\mathbf{x}}{ds} &= \dfrac{1}{|\mathbf{p}|}\mathbf{p}, \\[2mm] \dfrac{d\mathbf{p}}{ds} &= \vec{\nabla}\left(\dfrac{1}{v(\mathbf{x})}\right), \\[2mm] \dfrac{dT}{ds} &= \dfrac{1}{v(\mathbf{x})}, \end{cases} \qquad (7)$$

where $\mathbf{x}(s)$ denotes the position of the ray trajectory, while $\mathbf{p}(s)$ represents the slowness vector parameterized by the arc length s along the ray. The vector is tangent to the path of the ray at the point in isotropic media and orthogonal to the wavefront, satisfying the eikonal equation $|\mathbf{p}|^2 = 1/v^2(\mathbf{x})$. We can rewrite equation (7) in matricial form as

$$\frac{d\mathbf{y}}{ds} = \mathbf{f}(s, \mathbf{y}), \qquad (8)$$

where $\mathbf{y} = [\mathbf{x}, \mathbf{p}, T]$ and $\mathbf{f} = [\mathbf{p}/|\mathbf{p}|, -(1/v^2)\nabla v, 1/v]$. We discretize equation (8) using the fourth-order Runge-Kutta method with step length Δs, i.e., we consider $\mathbf{y}(n\Delta s) \approx \mathbf{y}_n$, where

$$\mathbf{y}_{n+1} = \mathbf{y}_n + \frac{1}{6}(\mathbf{k}_1 + 2\mathbf{k}_2 + 2\mathbf{k}_3 + \mathbf{k}_4), \qquad (9)$$

$$\begin{cases} \mathbf{k}_1 = \Delta s\mathbf{f}(s_n, \mathbf{y}_n), \\[1mm] \mathbf{k}_2 = \Delta s\mathbf{f}(s_n + \frac{1}{2}\Delta s, \mathbf{y}_n + \frac{1}{2}\mathbf{k}_1), \\[1mm] \mathbf{k}_3 = \Delta s\mathbf{f}(s_n + \frac{1}{2}\Delta s, \mathbf{y}_n + \frac{1}{2}\mathbf{k}_2), \\[1mm] \mathbf{k}_4 = \Delta s\mathbf{f}(s_n + \Delta s, \mathbf{y}_n + \mathbf{k}_3). \end{cases} \qquad (10)$$

After implementing and applying equation (10) over a parameterized velocity field, a polygonal trajectory is obtained that describes the path of the seismic ray. Within the iterative procedure of the Runge-Kutta method, the slowness vector, satisfying the eikonal equation, is always updated during the generation of segments, piece by piece, of the seismic trace. This same trace begins at $\mathbf{x}_0$ with a prescribed take-off direction, which defines the initial slowness $\mathbf{p}_0$, and set $T_0 = 0$. The path of the ray tends to bend as it encounters velocity variations, so that when starting from the source located on the surface, it travels a path in the subsurface and finds the receivers.

19

Traveltimes inversion procedure

In order to introduce seismic inversion in the traveltime calculation, we first consider a model vector **m** written as

$$\mathbf{m} = (m_1, m_2, m_3, \ldots, m_L)^T, \qquad (11)$$

and vector $\mathbf{d}^{obs} = (d_1, d_2, d_3, \ldots, d_K)^T$, associated with the following expression

$$e(\mathbf{m}) = \mathbf{d}^{obs} - \mathbf{g}(\mathbf{m}) = \mathbf{d}^{obs} - \mathbf{d}^{cal}.$$

Vectors $\mathbf{d}^{obs}$ and $\mathbf{d}^{cal}$ are the observed and calculated data on model **m**, defined as

$$\mathbf{d}^{obs} = (T_{obs}(\theta_1), T_{obs}(\theta_2), \ldots, T_{obs}(\theta_{N_r}))^T,$$

$$\mathbf{d}^{cal}(\mathbf{m}) = (T[\mathbf{m}](\theta_1), T[\mathbf{m}](\theta_2), \ldots, T[\mathbf{m}](\theta_{N_r}))^T, \qquad (12)$$

where $T_{obs}(\theta_i)$ and $T[\mathbf{m}](\theta_i)$ are the observed and calculated traveltime respectively, for the ray with take-off angle θ_i, while N_r is the number of rays that reach the surface in both cases. In order to compare the calculated data with the observed data we use the objective function defined in L^2-norm by

$$Misfit(\mathbf{m}) = \left[\frac{1}{N_r} \sum_{i=1}^{N_r} \left[\left(\frac{T[\mathbf{m}](\theta_i) - T_{obs}(\theta_i)}{T_{obs}(\theta_i)} \right)^2 \right. \right.$$
$$\left. \left. + \left(\frac{x(\theta_i) - x_{obs}(\theta_i)}{x_{obs}(\theta_i)} \right)^2 \right] \right]^{1/2}. \qquad (13)$$

The values that minimize equation (13) are computed using the genetic algorithm.

Overview of genetic algorithms

We are particularly interested in optimizing the objective function $Misfit$ defined by equation (13) aiming to obtain the velocity field **m**. In this case, an initial population is generated considering the limits of each parameter to be studied in the model. These parameters are usually encoded in binary strings, where each bit corresponds to a "gene" and each individual pattern in the population is described by its bit sequence or "chromosome". Conventionally, the chromosomes in an GA have a fixed length or scale. So when all bits are zero, the minimum value of the parameter is assumed, and when all bits are 1, the maximum value is assumed.

When GA optimization is initialized by random choice of parameters, the initial models with binary coding are then progressively optimized, maximizing the fitness function using the three biological evolutionary processes of *selection, crossover and mutation* until the best model adjustment is obtained. One of the characteristics of GA is its ability to work on a population of models simultaneously.

In "selection", the parameters are chosen according to their objective function values. In this step, we use the criterion of stochastic universal sampling (SUS) to select potentially useful parameters for recombination. Then, the crossover process is performed, where the selected models are paired and information is exchanged between each individual pair based on a probability. The crossover process was employed by the scattered technique, which consists of creating a random binary vector and selecting the genes where the digit 1 is from the first parent, and the genes where the digit 0 is from the second parent, and combining the genes to form a child. Finally, the "mutation" procedure adds noise from a Gaussian distribution with mean 0 to each entry of the parent vector to all parameters with low probability. The mutation helps to randomly change the position within the binary chain with some probability, preventing premature convergence. The mutation probability must be very low, otherwise the current good models will likely be destroyed. At the end of the mutation stage, the proposed new generations are accepted or rejected based on the Metropolis-Hastings rule, which is followed by the next cycle of genetic operations until some convergence measure is satisfied (HAJIAN; STYLES, 2018; SAMBRIDGE; MOSEGAARD, 2002). In Algorithm 1 we present a brief summary of the GA scheme in rectangular domain.

Below, we describe some advantages and disadvantages of the genetic algorithm:

Advantages:

1. The GA does not use local information, so it is not necessarily locked into local optima like gradient method.
2. Its performance is not affected by discontinuities in the function or its derivatives. The GA does not use derivative information in its evolution, so it does not need information from the gradients of the objective function surface to perform the search. This makes it very suitable for functions with discontinuities or for which we cannot calculate the derivative;
3. It is easy to implement and provides greater flexibility in dealing with the model problem;

Disadvantages:

1. Requires a large number of samples.

20

Semina: Ciênc. Ex. Tech., Londrina, v. 43, n. 1Esp, p. 17-28, Jan./Dez. 2022

Algorithm 1: GA scheme

Input:

Initialize chain by sampling from prior $\mathbf{m}^{(0)} = (m_1^{(0)}, \ldots, m_L^{(0)})^T \sim U(0,1)$ and crossover probability p_c;

$\mathbf{m} \leftarrow [v_{-1,-1}, \ldots, v_{N_x,N_z}]$;

for $k \in \{1, \ldots, N\}$ **do**

    $G_n(t) \leftarrow G_{0,n} \sqrt{y_l(t)}$;

    $v_a(x,z) \leftarrow \sum_{n=-1}^{N_z} \sum_{m=-1}^{N_x} v_{m,n} \phi_a\left(\frac{x}{h_x} - m\right) \phi_a\left(\frac{z}{h_z} - n\right)$;

    $\mathbf{m} \leftarrow [v_{-1,-1}, \ldots, v_{N_x,N_z}]$;

    Propose:

    One random vector θ^a,

    $u \sim U(0,1)$;

    if $u \leq p_c$ **then**

        select two individuals $\mathbf{m}, \mathbf{m}'$ from θ^a ;

        $\mathbf{m}^{(i)} \leftarrow \text{Crossover}(\mathbf{m}, \mathbf{m}')$;

        if $m^{(i)} \notin \{m, m'\}$ **then** evaluate $f(\mathbf{m}^{(i)})$ **else** infer $f(\mathbf{m}^{(i)})$ from parent;

    else

        select an individual $\mathbf{m}$ from θ^a;

        $\mathbf{m}^{(i)} \leftarrow \text{Mutation}(\mathbf{m})$;

        if $m^{(i)} \neq m$ **then** evaluate $f(\mathbf{m}^{(i)})$ **else** infer $f(\mathbf{m}^{(i)})$ from parent;

    end

end

Numerical experiments

The parameterization given by equation (4) will now serve as input data to the ray tracing algorithm. We compute the reference solution from the ray tracing procedure for discontinuous velocity models according to Červený (2001). The construction of a synthetic arrival is implemented by decompose the velocity field into subdomains such that the velocity is smooth within each subdomain, performing a ray tracing along which traveltime is calculated, until the ray strikes an interface. These steps are carried out until the stopping criterion is satisfied. In addition, we impose transmission conditions when the incidence angle at an interface is below the critical angle and reflection conditions otherwise.

The dimensions of the domain are fixed in $L_x = 9.4$ km and $L_z = 3.0$ km for all examples. In the examples below, the rays depart from $\mathbf{x}_0 = [x_0, z_0]$ with take-off angle θ with respect to the z-axis, $i.e.$, $\mathbf{p}_0 = [\sin(\theta), \cos(\theta)]/v_0$ (see Figure 1).

According to Oliveira et $al.$ (2021) we will consider the slope $a = 100$ to represent the velocity fields in the sigmoidal parameterization.

Finally, we need to choose a priori bounds $[\mathbf{m}_l^{min}, \mathbf{m}_l^{max}]$ in Algorithm 1 from the disturbance of the parameters of model $\mathbf{m}$. Here we stipulate the bounds for the velocity field $\mathbf{m}^{(0)} \in [0.8\mathbf{m}, 1.2\mathbf{m}]$ where $\mathbf{m}$

Figure 1 – Direction of the take-off angles in two dimensions
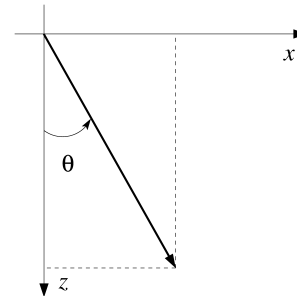
Source: Červený (2001).

is reference value from the velocity field. The initial population $\mathbf{m}^{(0)}$ is generated randomly. The algorithm computes the next generation of the samples using the fitness of the individuals in the current generation. As stopping criteria the GA is applied when it reaches the maximum number of generations M_G. In this case, the number of samples N used in the models presented depends on the number of parameters K according to the following equation:

$$N = \begin{cases} 100 + 47 \cdot (M_G - 1) & K < 10, \\ 400 + 190 \cdot (M_G - 1) & K \geq 10. \end{cases} \quad (14)$$

The present procedure was applied using the MATLAB® Optimization Toolbox. Additional parameters were left as MATLAB default values.

21

Semina: Ciênc. Ex. Tech., Londrina, v. 43, n. 1Esp, p. 17-28, Jan./Dez. 2022

In all our synthetic experiments, the forward responses obtained by the GA method are compared with the Simulated Annealing (SA) which is also a probabilistic technique for approximating the global optimum of a function (SEN; STOFFA, 2013). The SA is based on the physical process of heating a material whose temperature slowly drops to reduce the error, improving the approximation of the model. At each iteration of the SA, a new model is randomly generated. In this case, the initial temperature is $\mathbb{T}_0 = 100$ and the maximum number of iterations was fixed as the same as the number of iterations of the GA. Here the number of models tested by temperature is 10. Since

$$\Delta E = f(\tilde{\mathbf{m}}^{(k)}) - f(\mathbf{m}^{(k)}),$$

we update the model

$$\mathbf{m}^{(k)} \leftarrow \tilde{\mathbf{m}}^{(k)}$$

if $\Delta E \leq 0$ or if $\Delta E > 0$ and $P = \exp\left[-\Delta E/\mathbb{T}_i\right] > r$, where r is uniformly distributed ($r \sim U[0,1]$).

Horizontally layered model (M_1)

Let us consider the elementary one-dimensional model from Oliveira *et al.* (2021) of three horizontal layers of thickness $L = 0.75$ km and velocities $v_1 = 2.0$ km/s, $v_2 = 2.5$ km/s, and $v_3 = 3.0$ km/s with a single surface source at the origin as target model. The velocity below the third layer is $v_4 = 4.0$ km/s. In this inversion experiment we will try to estimate these four velocity parameters considering $M_G = 100$. In this experiment according to the stopping criterion on number of parameters, $N = 4,753$ samples were generated.

The arrival reflection locations $x^{(i)}$ and traveltimes $T^{(i)}$ ($i = 1, 2, 3$) for an arbitrary take-off angle θ are defined by

$$x^{(i)} = 2L \sum_{k=1}^{i} \tan\theta_k, \quad T^{(i)} = 2L \sum_{k=1}^{i} \frac{\sec\theta_k}{v_k}, \quad (15)$$

where $\theta_1 = \theta$ and $\theta_i = \sin^{-1}((v_i/v_{i-1})\sin\theta_{i-1})$ for $i = 2, 3$.

In Figure 2, we compare the ray paths of the inverted model using sigmoidal parameterization with reference solution, Figure 2(a), obtained from the discontinuous representation of the velocity field. An initial model was randomly generated in Figure 2(b). In addition, we evaluated the performance of GA and SA. In Figures 2(c)-(d) we can see that both methods have a similar plots and were able to successfully characterize the target model. The synthetic profiles of traveltime for an arbitrary take-off angle (continuous lines) and for the rays (dots) can be viewed through Figures 3(a)-(b).

Figure 2 – Reference solutions (a), initial model (b), inverted model by GA (c) and SA (d) methods for the horizontally layered model (M_1) with paths of 40 rays with take-off angles uniformly distributed in $[0°, 90°[$.

Source: The authors.

22

Semina: Ciênc. Ex. Tech., Londrina, v. 43, n. 1Esp, p. 17-28, Jan./Dez. 2022
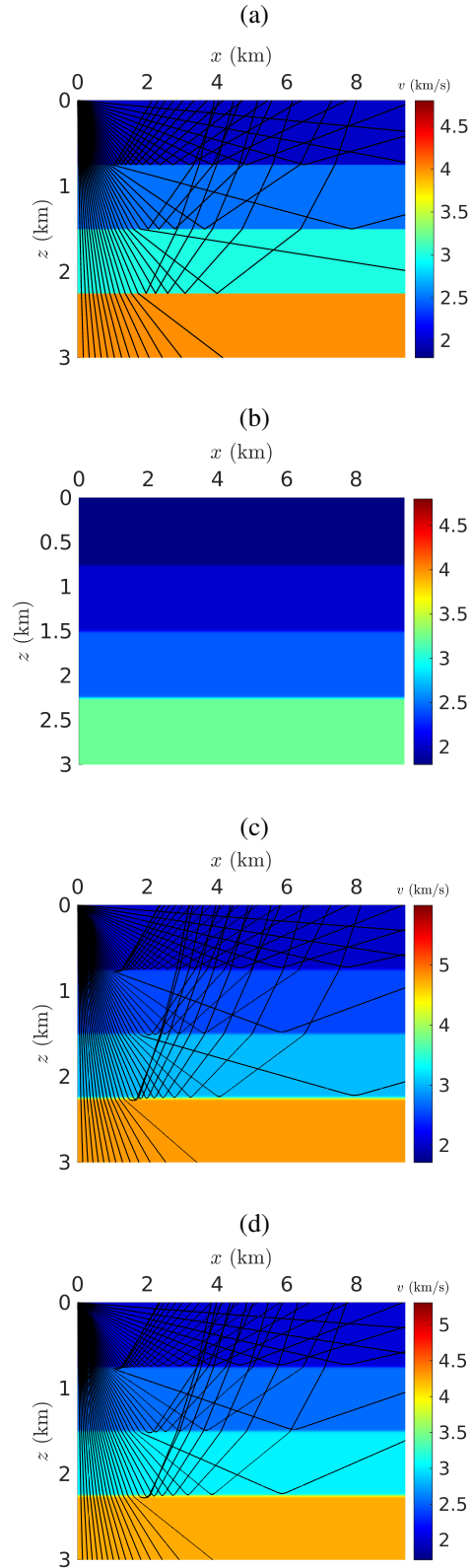
The inversion by sigmoidal functions has been able to detect with good approach the traveltime related to reflections from horizontal interfaces in both methods. However, GA had a slight advantage in approaching the traveltimes. In Figure 3(c) we plot the misfit between the inverted models and the target model M_1. We can infer that the results present an acceptable fit due to its low relative error. Table 1 presents the minimum misfit and CPU times for each method.

Figure 3 – Comparison between reference traveltime (Ref) for the horizontally layered model (M_1), with the ones found by sigmoidal approximations through the inverted model (Inv) obtained by GA (a) and SA (b) methods considering traveltimes of 200 rays. Plot of the misfit as a function of iteration number are illustrated in (c).

(a)

(b)

(c)
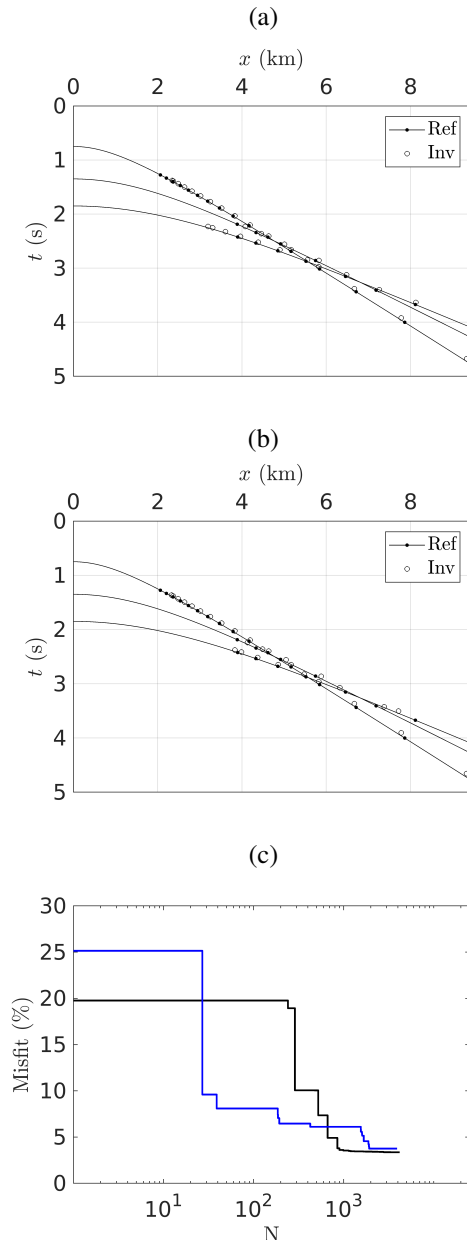
Source: The authors.

Table 1 – Misfit and CPU time for model M_1 considering GA and SA methods.

a	Method	Misfit	CPU (in seconds)
100	GA	0.0335	4.8560×10^3
	SA	0.0375	4.6685×10^3

Source: The authors.

High-velocity intrusion model (M_2)

The next synthetic test, we consider a representation of a laterally heterogeneous velocity field over a rectangular grid with 3×4 cells whose velocities vary from 1.5 km/s to 5.0 km/s, see Figures 4(a)-(b), to test the existing intrusion model against the new inversion model. According to the mesh size, this gives us 12 sigmoidal parameters to invert.

Figure 4 – A piecewise constant velocity model of a high-velocity intrusion model (M_2): 3D view (a) and the grid (b) defined by 3×4 cells.

(a)

(b)
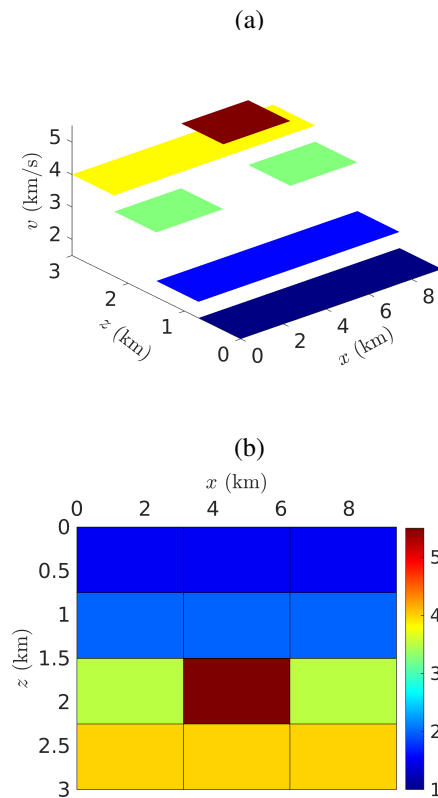
Source: The authors.

The ray paths in the velocity field and arrival times along with the initial model are plotted in Figure 5. In this case the arrangement consist of a single surface source located at $x_s = 4.65$ km with take-off angle θ uniformly distributed in $[-45°, 45°]$. In these figures we draw 40 rays to illustrate the ray trajectories through the model.

23

Semina: Ciênc. Ex. Tech., Londrina, v. 43, n. 1Esp, p. 17-28, Jan./Dez. 2022

Figure 5 – Reference solutions (a), initial model (b), inverted model by GA (c) and SA (d) methods for a high-velocity intrusion model (M_2) with paths of 40 rays. In pictures, the source point is located at (4.65 km, 0 km) and the take-off angles are uniformly distributed in $[-45°, 45°]$.

(a)

(b)

(c)

(d)
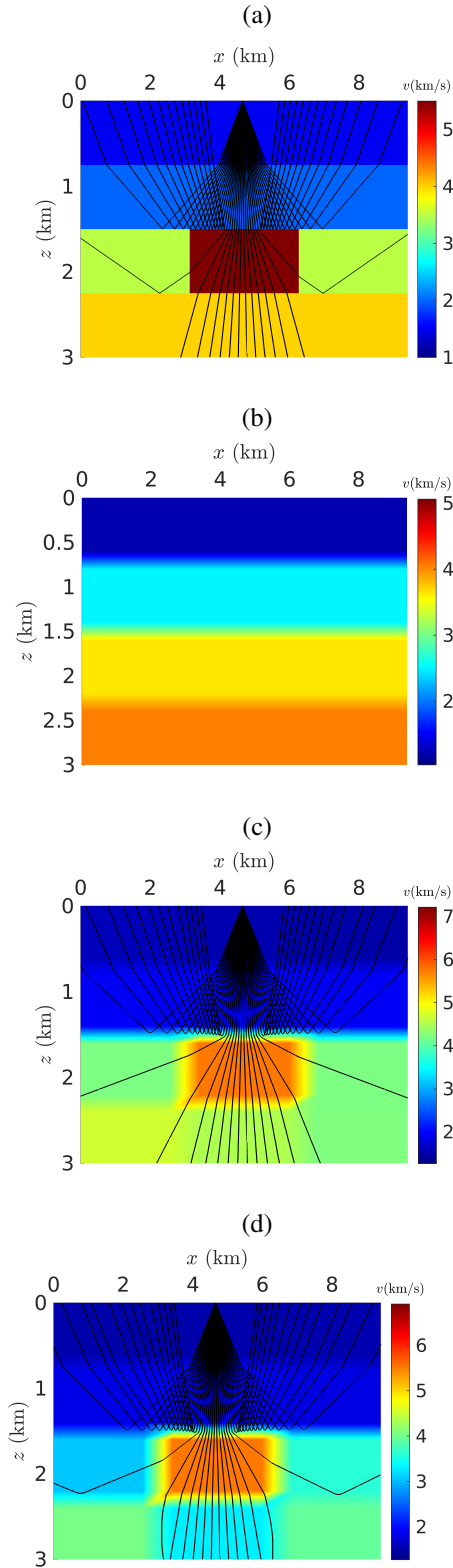
Source: The authors.

In the following, we compare ray paths obtained from GA and SA, Figures 5(c)-(d), with the target solution given by Figure 5(a). Due to the number of parameters, let us take $M_G = 100$ in GA. Both inverse models obtained for the sigmoidal parameterization described the intrusion region reasonably well and approached the target velocities with some accuracy. However, the GA has an advantage because it better characterizes the regions that suffer from the change in velocity. For the two methods under study, approximately $N = 19,210$ realizations of data sets were generated.

On the other hand, in Figures 6(a)-(b) we employ 200 rays with take-off angles uniformly distributed in the same interval to compute traveltimes. We also use the misfit in this example for the purpose of comparing the inverted model obtained by GA and SA, plotted in Figure 6(c). Although the result of the inversion was not optimal, the traveltimes had a good approximation in most of the GA model, keeping the error below 5%, while the traveltimes defined by the SA model had a slight deviation from the target traveltimes. Also note that the SA has a higher misfit among the number of tests with error $\approx 10\%$. In addition, Table 2 summarizes the superiority of GA over SA. The result presented by misfit had a lower value in the GA method despite a slight gain in CPU time in the SA method.

Table 2 – Misfit and CPU time for model M_2 considering GA and SA methods.

a	Method	Misfit	CPU (in seconds)
100	GA	0.0431	9.4728×10^4
	SA	0.0962	8.4422×10^4

Source: The authors.

Sedimentary sequence model (M_3)

The following synthetic test considers a representation of a laterally heterogeneous velocity field over a rectangular grid with 12×12 cells whose velocities vary from 1.5 km/s to 5.0 km/s and are assumed constant within each of these cells, see Figures 7(a)-(b). According to the mesh size, this gives us 144 sigmoidal parameters to invert. Unlike the M_1 and M_2 models, the arrangement consist of ten sources, uniformly spaced with take-off angle θ uniformly distributed in $[-45°, 45°]$ and 200 receivers equally spaced totaling 200 recorded traveltimes per source, uniformly spaced, and we take $M_G = 300$. In both methods, $N = 57,210$ models were generated.

24

Semina: Ciênc. Ex. Tech., Londrina, v. 43, n. 1Esp, p. 17-28, Jan./Dez. 2022

Figure 6 – Comparison between reference traveltimes (Ref) for a high-velocity intrusion model (M_2), with the ones found by sigmoidal approximations through the inverted model (Inv) obtained by GA (a) and SA (b) methods considering traveltimes of 200 rays. Plot of the misfit as a function of iteration number are illustrated in (c).

(a)

(b)

(c)
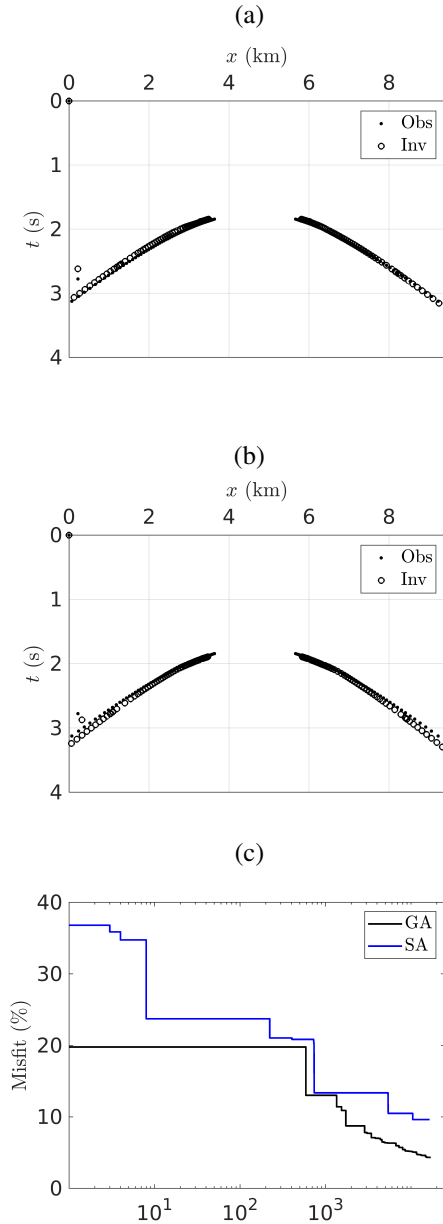
The ray paths in the target velocity field and arrival times are plotted in Figure 8(a).

Similar to the M_2 model, in order to compare these results with the SA, we proposed an initial velocity field model for both methods, see Figure 8(b). As shown in Figures 8(c)-(d), the models obtained by the inversion are not sufficiently close to the reference model, but certain characteristics can already be noticed in the GA, such as: the dip of the layers, the growth of velocities with the

Figure 7 – A piecewise constant velocity model of a sedimentary sequence slope (Model M_3): 3D view (a) and the grid (b) defined by 12×12 cells.

(a)

(b)
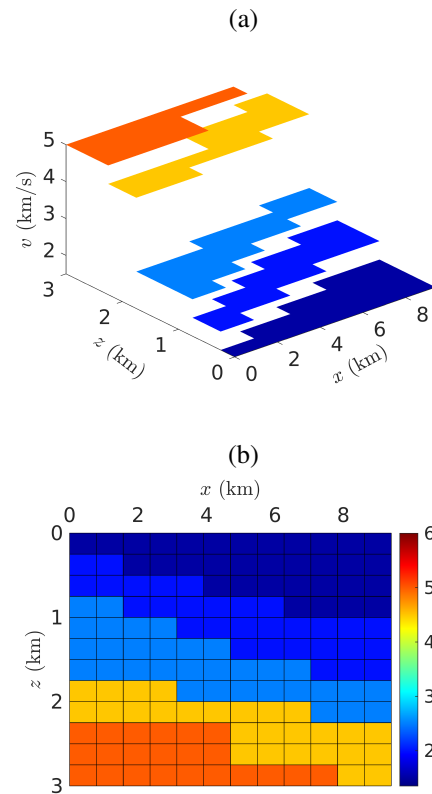
depth and the permanence of these within the established range, unlike the SA that did not characterize these details in the velocity model.

In Figures 9(a)-(b) we only plot traveltimes from two sources for better visualization. Due to the inaccuracy of the velocity field in some cells, the traveltimes computed by the inversion using the GA did not have a close approximation, see Figure 9(a). This result is confirmed in the misfit values as observed and compared with the SA in Table 3 and Figure 9(c).

Table 3 – Misfit and CPU time for model M_3 considering GA and SA methods.

a	Method	Misfit	CPU (in seconds)
100	GA	0.8338	6.9754×10^5
	SA	1.7357	6.6334×10^5

25

Semina: Ciênc. Ex. Tech., Londrina, v. 43, n. 1Esp, p. 17-28, Jan./Dez. 2022

Figure 8 – Reference solutions (a), initial model (b), inverted model by GA (c) and SA (d) methods for a high-velocity intrusion model (M_3) with paths of 10 rays per source. In pictures, the source point are uniformly spaced and the take-off angles are uniformly distributed in $[-45°, 45°]$.

(a)

(b)

(c)

(d)
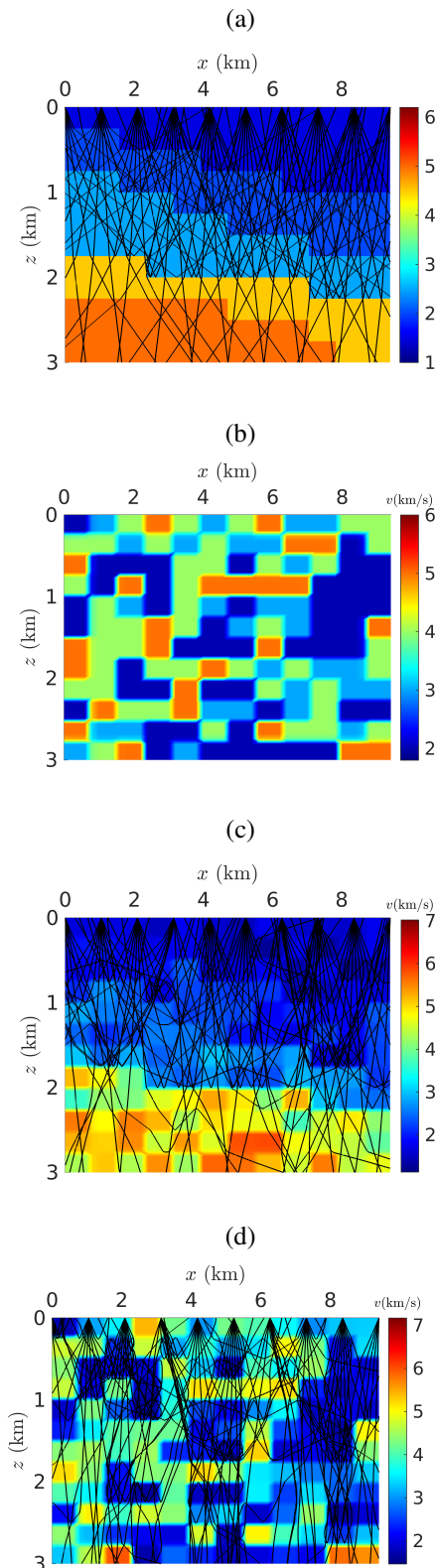
Source: The authors.

Figure 9 – Comparison between reference traveltimes (Ref) for a high-velocity intrusion model (M_3), with the ones found by sigmoidal approximations through the inverted model (Inv) obtained by GA (a) and SA (b) methods considering traveltimes of 200 rays. Here we plot the traveltimes from two sources located in $[2.1, 0.0]$ and $[7.3, 0.0]$. Plot of the misfit as a function of iteration number are illustrated in (c).

(a)

(b)

(c)
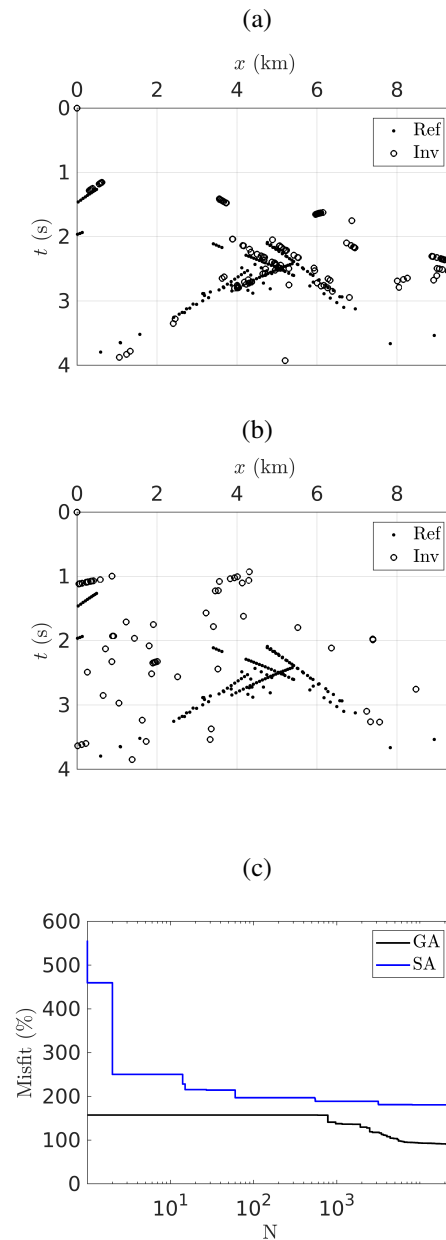
Source: The authors.

Discussion and conclusion

The genetic algorithm proved to be effective in generating velocity fields that remained within the velocity ranges corresponding to the original models and approached reasonably well.

26

Semina: Ciênc. Ex. Tech., Londrina, v. 43, n. 1Esp, p. 17-28, Jan./Dez. 2022

During the inversion process, even with the increase in parameters, the adopted methodology did not require a high computational cost. In addition, the results of the parameterized velocity fields remained reasonably close.The experiments with the M_1 model generated very good results, both quantitatively and qualitatively. The higher quality of these results, compared to the other experiments, is probably due to the low number of parameters involved in the direct modeling step. Note that the observed changes regarding the number of parameters have an effect on the calculation of traveltimes. This is observed in the experiments given by the models M_2 and M_3. The inverse M_2 model was able to reproduce the traveltime curve with some accuracy in relation to the target solution, which did not happen with the M_3 model. Due to the increase in the number of parameters in the M3 model, we consider to increase the number of sources and generations M_G to better characterize the velocity field in the inversion. Note that the SA algorithm was not able to clearly capture distinct regions of the velocity field, while in the GA we had a better identification. In short, GA showed better performance in all experiments compared with SA. Despite the natural increase in misfit with the number of parameters, the results provided by GA can be good candidates for initial models to be used by local search or hybrid methods.

References

BOZDAĞ, E.; TRAMPERT, J.; TROMP, J. Misfit functions for full waveform inversion based on instantaneous phase and envelope measurements. *Geophysical Journal International*, Oxford, v. 185, n. 2, p. 845–870, 2011.

CERQUEIRA, A. G.; FIGUEIRÓ, W. M.; CUNHA, P. E. M. Seismic tomography using metropolis method of velocity fields parameterized by Haar wavelet series. *Revista Brasileira de Geofísica*, São Paulo, v. 34, n. 2, p. 251–260, 2016.

ČERVENÝ, V. *Seismic Ray Theory*. Cambridge: Cambridge University Press, 2001.

DATTA, D.; SEN, M. K. Estimating a starting model for full-waveform inversion using a global optimization method. *Geophysics*, Tulsa, v. 81, n. 4, p. R211–R223, 2016.

DOCHERTY, P.; SILVA, R.; SINGH, S.; SONG, Z.-M.; WOOD, M. Migration velocity analysis using a genetic algorithm. *Geophysical Prospecting*, Oxford, v. 45, n. 5, p. 865–878, 1997.

ELY, G.; MALCOLM, A.; POLIANNIKOV, O. V. Assessing uncertainties in velocity models and images with a fast nonlinear uncertainty quantification method. *Geophysics*, Tulsa, v. 83, n. 2, p. R63–R75, 2018.

FERREIRA, N. R.; PORSANI, M. J.; OLIVEIRA, S. P. A hybrid genetic-linear algorithm for 2d inversion of sets of vertical electrical sounding. *Revista Brasileira de Geofísica*, São Paulo, v. 21, p. 235–248, 2003.

HAJIAN, A.; STYLES, P. *Application of soft computing and intelligent methods in geophysics*. Berlin: Springer, 2018.

HANYGA, A.; SEREDYŃSKA, M. Ray tracing in elastic and viscoelastic media. *Pure and Applied Geophysics*, Basel, v. 157, n. 5, p. 679–717, 2000.

JIN, C.; CAO, D.; YIN, X. Joint waveform inversion with the separated upgoing and downgoing wavefields of VSP data. *Journal of Geophysics and Engineering*, Oxford, v. 17, n. 1, p. 53–64, 2020.

MENKE, W. *Geophysical data analysis*: discrete inverse theory: MATLAB edition. Cambridge: Academic press, 2012. v. 45.

MOLLEHUARA-CANALES, R.; KOZLOVSKAYA, E.; LUNKKA, J.; MOISIO, K.; PEDRETTI, D. Non-invasive geophysical imaging and facies analysis in mining tailings. *Journal of Applied Geophysics*, Amsterdam, v. 192, p. 104402, 2021.

OLIVEIRA, S. P.; AZEVEDO, J. S.; FIGUEIRÓ, W. M.; GUIMARÃES, R. A.; SILVA, W. J.; OLIVEIRA, A. Representation of discontinuous seismic velocity fields by sigmoidal functions for ray tracing and traveltime modelling. *Geophysical Journal International*, Oxford, v. 224, n. 1, p. 435–448, 2021.

RAWLINSON, N.; FICHTNER, A.; SAMBRIDGE, M.; YOUNG, M. K. Seismic tomography and the assessment of uncertainty. *Advances in geophysics*, New York, v. 55, p. 1–76, 2014.

REZAIE, M. A sigmoid stabilizing function for fast sparse 3d inversion of magnetic data. *Near Surface Geophysics*, Houton, v. 18, n. 2, p. 149–159, 2020.

SAJEVA, A.; ALEARDI, M.; STUCCHI, E.; BIENATI, N.; MAZZOTTI, A. Estimation of acoustic macro models using a genetic full-waveform inversion: Applications to the Marmousi model. *Geophysics*, Tulsa, v. 81, n. 4, p. R173–R184, 2016.

SAMBRIDGE, M.; DRIJKONINGEN, G. Genetic algorithms in seismic waveform inversion. *Geophysical Journal International*, Oxford, v. 109, n. 2, p. 323–342, 1992.

SAMBRIDGE, M.; MOSEGAARD, K. Monte Carlo methods in geophysical inverse problems. *Reviews of Geophysics*, Washington, v. 40, n. 3, p. 3–1, 2002.

SEN, M. K.; STOFFA, P. L. *Global optimization methods in geophysical inversion*. 2. ed. Cambridge: Cambridge University Press, 2013.

STUART, G. K.; MINKOFF, S. E.; PEREIRA, F. A two-stage Markov chain Monte Carlo method for seismic inversion and uncertainty quantification. *Geophysics*, Tulsa, v. 84, n. 6, p. R1003–R1020, 2019.

28

Semina: Ciênc. Ex. Tech., Londrina, v. 43, n. 1Esp, p. 17-28, Jan./Dez. 2022